*International Journal of Advanced Engineering Research and Science (IJAERS)*
*Peer-Reviewed Journal*
*ISSN: 2349-6495(P) | 2456-1908(O)*
*Vol-9, Issue-5; May, 2022*
*Journal Home Page Available: https://ijaers.com/*
*Article DOI: https://dx.doi.org/10.22161/ijaers.95.16*

# Relationship between soil management and rainfall erosion: A case study in the Guajará-Mirim river watershed, Vigia - Pará

Jaime Carvalho Goes[1], Eder Silva de Oliveira[2]

[1]Department of Environmental and Sanitary Engineering, State University of Pará, Brazil
Email: jaime.goes@aluno.uepa.br
[2] Department of Environmental and Sanitary Engineering, State University of Pará, Brazil
Email: ederso@uepa.br

Received: 16 Apr 2022,

Received in revised form: 13 May 2022,

Accepted: 18 May 2022,

Available online: 23 May 2022



***Keywords*— Ground cover, Pluvial erosion, QGIS, Remote sensing, USLE.**

***Abstract*— *This study aims to evaluate the relationship between soil management and its loss by rainfall erosion in the watershed of the Guajará-Mirim river. The methodology used was essentially carried out by remote sensing, literature review and the application of the Universal Soil Loss Equation (USLE), with the geoprocessing of matrix and vector files in the QGIS software. The results show that, in relation to soil management in the study region, considering that it is a plain and that there were no measures to control soil erosion, its loss by rainwater transport is aggravated the greater the exposure of the soil, that is, the removal of vegetation and the revolving soil horizons. This assertion is evidenced by the greater soil loss in the areas mapped for sand extraction and deforestation by calculating the Universal Soil Loss Equation.***

## I. INTRODUCTION

According to the provisions of item II, article 3 of the National Environmental Policy [1], the degradation of environmental quality consists of adverse changes in the characteristics of the environment. Such unfavorable alteration may have a natural or anthropic origin. In cases where the origin is natural, it can be said that unavoidable disasters or losses have occurred. Otherwise, when degradation is caused by human intervention, the loss of environmental quality would be avoidable and the human being assumes the role of responsible for altering the quality of the environment, which may or may not exceed its capacity for natural self-recovery [2].

The process of soil erosion consists of the disaggregation, transport and deposition of parts of the soil, whether small grains or larger amounts, and may be caused by the action of natural agents, mainly water and wind, or by human pressure. Water erosion caused by rainfall is one of the main causes of soil fertility loss, being observed mainly in areas with high rainfall, exposed soil and uneven topography. Wind erosion is related to arid and semi-arid climate zones that present exposed soil, both in plains and in irregular reliefs [3].

From a physical point of view, what causes soil loss due to rainfall erosion is the impact of the raindrop against the soil (splash) and the surface runoff of water (soil drag). The susceptibility to erosion of an area depends on certain physical characteristics, which include the nature of the soil (texture, structure and porosity), the rainfall rate of the region, relief and soil cover [3].

It has been developed about water erosion in hydrographic basins in order to estimate the soil loss caused by the action of rain over time. This measurement can help in decision-making in soil management plans, and one of the main ways of calculating to estimate soil loss from rainfall erosion is the Universal Soil Loss Equation [4], [5].

Deforestation and fires with a view to agricultural and logging use are among the human causes that aggravate soil erosion by the action of rain, reducing the amount of organic matter in the surface layers of the soil, as well as losses in the aggregation between particles and a drop in fertility [6].

The intensive use of agricultural equipment and grazing are also potential factors for increasing soil erosion, as they leave the soil compacted and with little vegetation cover. Mineral exploration in an environmentally unregulated manner is also a factor to be considered, since soil disturbance and exposure to physical weather favor the leaching process, and the risk of leakage in ore tailings dams must also be considered [2].

Geographic Information Systems (GIS) currently represent a set of computational tools of great use for professionals in the environmental area [7]. They specialize in acquiring, storing, retrieving, transforming and issuing geospatial information. Your data depict real objects in terms of cartographic position, non-apparent attributes, and topological relationships. A GIS can be used in environmental studies, in the prediction of certain phenomena and in supporting planning decisions, considering the concept that the stored data represent a model of the real world [8].

Among the most used geoprocessing software today, QGIS stands out in this work for its relevance in the academic and professional environment, being characterized as free, open source (programmers can contribute to its improvement with new tools) and have regular updates [9].

Therefore, as in the Guajará-Mirim river microbasin area, there are several land uses with different potential for rainfall erosion and, in view of the importance of preserving soil quality, an attempt was made to classify and quantify the land cover areas and their respective losses from rainfall erosion through the application of the USLE in the QGIS software.

This study evaluated the relationship between soil management and its loss by rain, in the watershed located on the banks of the Guajará-Mirim river, Vigia - PA, through the application of the Universal Soil Loss Equation (USLE) in the geoprocessing software. QGIS .

## II. THEORETICAL REFERENCE

2.1 Photointerpretation

The use of satellite images, in the scope of geotechnologies, is invariably related to the process of photointerpretation of the identifiable categories in the area of interest. Satellite and drone images allow a detailed analysis of the ground surface and are treated in Geographic Information Systems (GIS). The affirmation of this type of analysis depends on the spatial resolution of the satellite images, as well as the technician's ability to visually recognize the land uses of the specific region [10].

The classes of soil cover or use and occupation may vary according to the scope of the study and the nomenclature adopted, and they generally involve: native vegetation; secondary vegetation; agriculture; clean pasture; dirty pasture; logging; burned; hydrography; rock formation; wooded areas; anthropized, civil construction and industrial areas [7].

2.2 Universal Soil Loss Equation (EUPS)

The Universal Soil Loss Equation - EUPS was developed by assistant scientists at the US Department of Agriculture [4], [5]. Its purpose is to predict the long-term average rate of soil erosion using six physical variables (1). It should be noted that its application is intended to calculate the loss of soil from laminar erosion or surface furrows, its formulation does not predict river bed erosion, as well as other more severe forms of erosion, such as ravines and gullies [11].

$$A = R\,K\,LS\,C\,P \qquad (1)$$

Where: A is the estimated soil loss in ton per hectare per year ($t\ ha^{-1}\ year^{-1}$);

R is the rainfall erosivity factor, the potential for rainfall to cause erosion ($MJ\ mm\ ha^{-1}\ h^{-1}\ year^{-1}$);

K is the soil erodibility factor, the ability of the soil to resist the erosive process ($t\ h\ MJ^{-1}\ mm^{-1}$);

LS is the topographic terrain factor, taking into account the ramp length (L) and the terrain slope factor (S), dimensionless;

C is the land use and management factor, proportional to the type of cover that is on the ground (dimensionless);

P is the conservation practices factor, it identifies erosion control measures applied in the region of interest (dimensionless).

## III. METHODOLOGY

3.1 Study area

The study area is the Guajará-Mirim river watershed, located in the central region of the municipality of Vigia, in the state of Pará. According to Faustino [12], hydrographic sub-basins are drainage areas of the tributaries of the main watercourse, ranging from 100 km² to 700 km². To a lesser extent, a microbasin has a drainage area to the main river of the sub-basin and an area of less than 100 km² [12]. Therefore, several watersheds form a sub-basin. The study area fits as a watershed because it has an area estimated by remote sensing of 96,541 km²

The estimated population in 2021 in the municipality of Vigia (PA) is 54,650 inhabitants, with a territorial area of 401,589 km² and a population density of 88.83 inhab/km². In livestock, the local economy stands out for the tambaqui aquaculture, for the creation of cattle and chicken herds and for the cultivation of honey, in addition to breeding buffaloes, goats, horses, sheep and pigs [13].

Vigia integrates the mesoregion of Northeast Pará and the microregion of Salgado, forming part of the Amazon biome [13]. According to Kottek et al. [14] the municipality is included in the Köppen climate classification, presenting a tropical monsoon climate (Am), with a brief dry season and an average annual rainfall that can vary from 1750 to 3000 millimeters.

The cartographic scale of Figure 1 refers to the main map of the study area, the secondary map of the location of the municipality is illustrative.

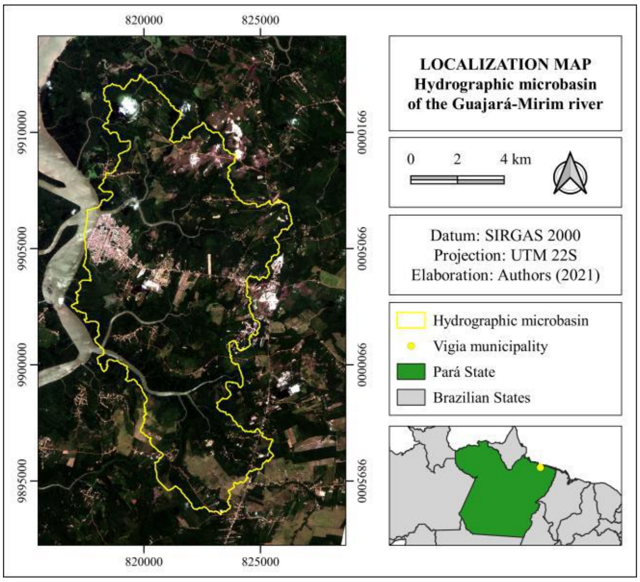


*Fig. 1. Location map of the Guajará-Mirim river watershed in Vigia (PA).*

3.2 Software, satellite image and vector base

The elaboration of thematic maps was performed in the geoprocessing software QGIS 3.16.8 Hannover. For the location map of the watershed, a scene from the CBERS 04A satellite was used, with a capture date on 08/20/2020, quadrant 211/114 (Path/Row). For the selection of the best image in the Image Generation Division [15] the one with better visibility, less presence of clouds and the most recent imaging date, with temporal resolution from 01/01/2020 to 07/31/ 2021. The cartographic bases of the municipalities and states used were the IBGE [13]

3.3 Composition of CBERS 04A satellite spectral bands

The image composition in natural colors of the CBERS 04A satellite was made in the QGIS 3.16.8 Hannover software, through the composition of bands 3 (red), 2 (green) and 1 (blue) of 8 meters of resolution, with band 0 (panchromatic) of 2 meters of resolution, improving the spatial resolution of the image from 8 to 2 meters in the area of interest [16].

3.4 Correction of the Digital Elevation Model

One of the necessary input data for the elaboration of USLE thematic maps is an altitude raster. It took 4 quadrants to fully cover the area of interest, obtained from the Topodata project website, which provides 30-meter spatial resolution SRTM (Shuttle Radar Topography Mission) radar images: 00S495, 01S495, 00S48 and 01S48 [17]

An altitude raster usually presents imperfections in its primary state, as there is no perfect digital elevation model, given the complexity of the earth's surface and the level of geometric fidelity that geoprocessing software provides, but there are technically acceptable models. To alleviate the imperfections, three processes were necessary: the removal of negative altitude values [18]; filling in the pixels without data (tiny blank spaces) [19]; and the leveling of spurious depressions (pixels with incongruent values in relation to their immediate altimetric neighborhood [20].

To correct the negative altitude values, the Raster Calculator function of the SAGA (System for Automated Geoscientific Analyses) in QGIS was used, with the input of the formula: “ifelse (a<0, 0, a)”, which considers negative values as zero altitude and maintains the other values [18],[21].

To fill in the tiny blank spaces, we used the Fill no data function, with the default setting. In this way, the software fills the blank values with values that are in accordance with the most likely statistic of the pixel neighborhood [19]

To correct the spurious depressions, SAGA's Fill sinks (Wang & Liu) tool was used, which flattens the altitude of pixels with outliers. After these technical procedures, there is a Hydrologically Consistent Digital Elevation Model (HCDEM), with altimetric values closer to reality [20]

### 3.5 Rain Erosivity Factor (R)

The method of calculating the factor R proposed by Lombardi Neto and Moldenhauer [22] was implemented, which arrived at Equation 2, derived from the regression between the average monthly erosion index and the rainfall coefficient.

$$EI_{mensal} = 68{,}730\left(\frac{p^2}{P}\right)^{0{,}841} \tag{2}$$

Where: EI is the monthly average of the erosion index (MJ.mm/ha.h.year);

p indicates the average monthly rainfall (mm);

P indicates the average annual precipitation (mm).

To obtain the annual rainfall erosivity factor, it is necessary to calculate the average of the EI values for the 12 months of the year (3). The historical series used was from the years 1990 to 2020. The average of R was calculated for each sample year and the average of 31 years (4), which is the final value considered for the map algebra (R factor of USLE). The data used were downloaded from the Hidroweb platform of the National Water Agency [23], selecting the rainfall station in Vigia (PA). The calculation of the mentioned formulas was done in the Excel 2019 program [22].

$$R_{anual} = \frac{\sum_{i=1}^{12} EI(i)_{mensal}}{12} \tag{3}$$

$$R_{final} = \frac{\sum_{i=1}^{31} R(i)_{anual}}{31} \tag{4}$$

### 3.6 Soil Erodibility Factor (K)

The soil erodibility factor K depends on the geological knowledge of the soil in question. According to the Soil Map of Brazil [24], the Guajará-Mirim river watershed in Vigia (PA) is predominantly located in the patch of dystrophic yellow latosol of medium texture, with pedological formations of dystrophic concretionary petric plintosol and neosol orthic quartzarenic.

According to the Geodiversity Cartographic Survey of the State of Pará [25], the watershed of the Guajará-Mirim River is part of the lithological formation of Post-Barreiras Sediments. It has a characteristic presence of consolidated and semi-consolidated sands, yellowish cream and white, with fine to medium granulometry, containing a fraction of clay and millimetric quartz clasts. In a field survey in the area, the authors of the present study found the presence of quartzarenic neosols in the sand mineral extraction areas.

### 3.7 Topographic Factor (LS)

The method applied in the QGIS 3.16.8 software to calculate the LS topographic factor was carried out using the field-based SAGA (System for Automated Geoscientific Analyses) Factor LS tool. A Digital Elevation Model (DEM) is required as input, and catchment areas are derived according to Freeman's computational model, being used instead of the slope factor originating from the EUPS [26], [21].

As a DEM with a spatial resolution of 30 meters was inserted [17], the resulting raster has this same characteristic. The selected LS topographic factor equation that allowed automatic calculation in QGIS was developed and described by Desmet and Govers [27].

### 3.8 Soil Cover Factor (C)

The soil cover classes were identified in the Guajará-Mirim river microbasin through photointerpretation and manual vectorization in the QGIS 3.16.8 software and comparison with the classes from the shapefile provided by ESRI, Use and Occupation of Soil of Globo Terrestre for the year of 2020, with a spatial resolution of 10 meters [28]. The soil cover classes adopted and identified were: native vegetation, secondary vegetation, clean pasture, dirty pasture, hydrography, dam, anthropized area, deforestation and mineral extraction. An attempt was made to use nomenclatures similar to those of the TerraClass Project by Embrapa [29].

The native vegetation is characterized by the presence of dense forest and closed canopy, presenting predominantly dark green coloration, with no identifiable water courses below this vegetation by the orthogonal view. The secondary vegetation is characterized by shrubs, few tall trees and a canopy of lower height than the native vegetation, with a predominant medium green color [28],[29].

Clean pasture can be seen in areas with a low presence of shrubby vegetation, associated with the creation of herds, homogeneous grasses with little or no higher vegetation; may have wild cereals, without human planting. Grass is characterized by areas that may have previously been used for grazing and are undergoing an ecological succession process, or areas that have been degraded for some time and have begun to recover naturally; are fields with little or no tree cover, but which already have some surface cover greater than that of clean pasture, such as sparse shrubs and tall grass [28],[29].

The hydrography is characterized by the presence of the Guajará-Mirim river and its tributaries, meanders that can reach up to 10 meters in width, in addition to some ponds with still water, being small lakes of dark water that normally serve for recreation or animal watering. The category of anthropized area comprises the nuclei of residences and buildings, mainly in the central part of the municipality of Vigia. As it is a municipality with a large presence of rural areas, some houses are in very close contact with native and secondary vegetation. In the photointerpretation, only those areas with significant soil impermeabilization were considered as anthropized areas, mainly in the central area of the municipality [28],[29].

Areas of deforestation were identified by the presence of clearings in the midst of native or secondary vegetation, in locations where no connection between the clearings and the presence of anthropized areas was identified, implying that this is possibly an area that suffered clear-cutting of wood. The areas of mineral extraction of sand are easily identified by satellite image due to their white-yellowish tone, different from the other land cover classes [28],[29].

After vectorizing the entire area of interest, the Rasterize operation in QGIS was necessary to convert the files in shapefile (vector) to raster (matrix) format, so that it can be used in map algebra. Inverse operation was performed on the final raster of soil loss due to rainfall erosion (Vectorize), the values of each pixel of 30 meters were extracted in the form of vector points, for the calculation of soil loss by cover class.

## IV. RESULTS AND DISCUSSION

### 4.1 Rain Erosivity Factor (R)

According to the defined methodology, the result of the Rfinal factor, which is used in the algebra of the equation A = R K LS C P, was approximately 682 MJ.mm/ha.h.year [22]. This value numerically represents the average rainfall erosivity factor, considering the sampling interval of 31 years adopted and the rainfall data from the Vigia meteorological station [23].

*Table 1. $R_{final}$ value.*

| $R_{final}$ | Unit |
|---|---|
| 682 | MJ.mm/ha.h.year |

According to Silva et al. [30], this is an R factor considered of weak erosivity, according to the classification Table 2. This shows that the region, characterized as a plain, with little altimetric variation and being located in the equatorial zone of the globe (IBGE, 2021b), presented a weak potential for rainfall erosivity throughout the historical series of analysis.

*Table 2. R values according to the levels of rainfall erosivity, in MJ mm $ha^{-1}$ $h^{-1}$.*

| R Factor | Erosivity |
|---|---|
| < 2452 | Weak |
| 2452 – 4905 | Medium |
| 4905 – 7357 | Medium to Strong |
| 7357 – 9810 | Strong |
| > 9810 | Very Strong |

*Source: Silva et al. (2003).*

### 4.2 Soil Erodibility Factor (K)

Silva and Alvares [31], carried out a review of K values for soil classes in the state of São Paulo, finding mean values for soil classes similar to those found in the Guajará-Mirim river watershed. The soil cover classes were classified as dystrophic yellow latosol: native vegetation, secondary vegetation, dirty pasture, clean pasture, agriculture and deforestation. For the areas photointerpreted as sand extraction, quartzarenic neosols were considered. The classes of anthropic area, hydrography and weir did not receive soil erodibility values, since they do not fit the K-factor erosion measurement criterion (Table 3).

It is noteworthy to evaluate the K factor that the quartzarenic neosols present in the basin area have a sandy texture along the profile, with a very reduced A horizon, it is in these soils that the activities of sand extraction are carried out. The dystrophic yellow latosols present conditions of good water retention, good permeability and sandy-clay texture, where all agricultural practices in the area are developed.

*Table 3. Values for the Erodibility Factor K, in $t.ha^{-1}.MJ^{-1}.mm^{-1}$.*

| Soil Class | K Factor |
|---|---|
| Dystrophic yellow latosol | 0.0043 |
| Quartzarenic neosol | 0.0127 |

*Source: Silva e Alvares [31].*

According to the classification proposed by Silva et al. [30], the soil classes identified in the Guajará-Mirim river watershed have low soil erodibility values. The higher the value for K, the lower the natural resistance of the soil structure to rainfall erosion (Table 4).

*Table 4. Soil Erodibility Potential, in t ha $MJ^{-1}$ $mm^{-1}$.*

| K Factor | Erodibility |
|---|---|
| < 1.471 | Low |
| 1.471 – 2.943 | Medium |
| > 2.943 | High |

*Source: Silva et al. [30].*

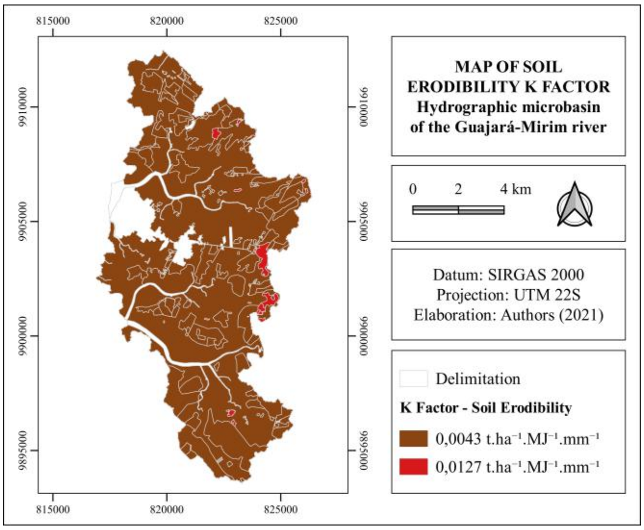


*Fig. 2. Soil Erodibility K Factor Map.*

4.3 Topographic Factor (LS)

According to the resulting calculations, the LS topographic factor presented values ranging between 0.03 and 17.41 in the Guajará-Mirim river watershed, with most of the area not exceeding 2.50. Values above 2.50 are linked to river slope areas. The higher the LS topographic factor, the greater the susceptibility of the region to the occurrence of erosion, as the slope of the terrain favors the dragging of soil by the rains [11].

*Table 5. Slope Classes.*

| Slope (%) | Relief |
|---|---|
| 0 – 3 | Plan |
| 3 – 8 | Soft-wavy |
| 8 – 20 | Wavy |
| 20 – 45 | Strong-wavy |
| 45 – 75 | Mountainous |
| > 75 | Strong-mountain |

*Source: Embrapa [32].*

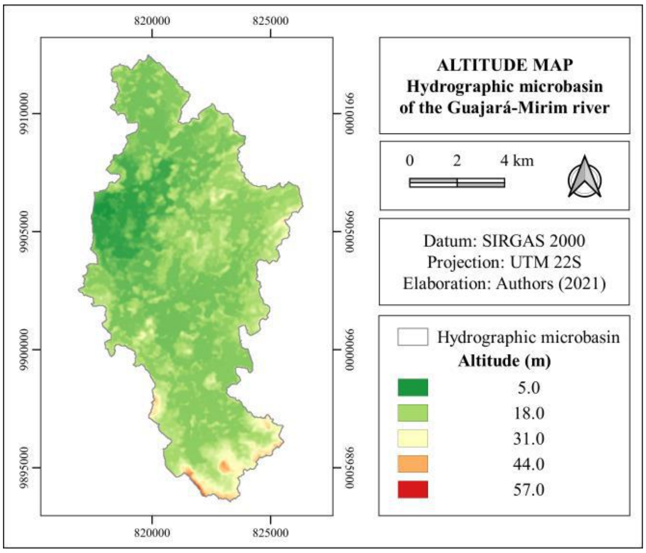


*Fig. 3. Altitude Map.*

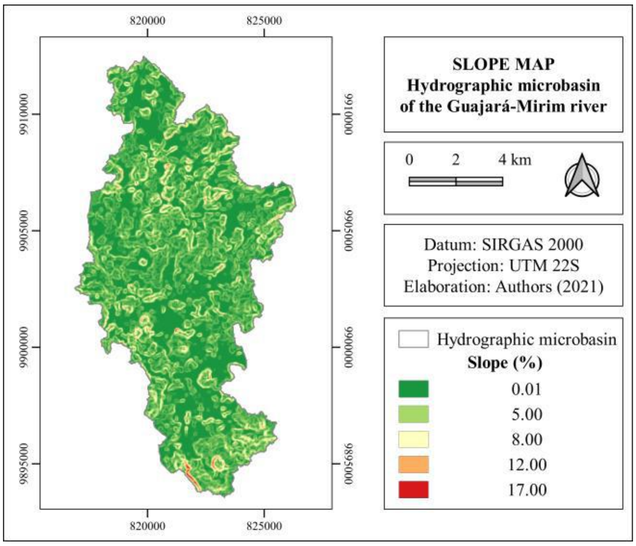


*Fig. 4. Slope Map.*

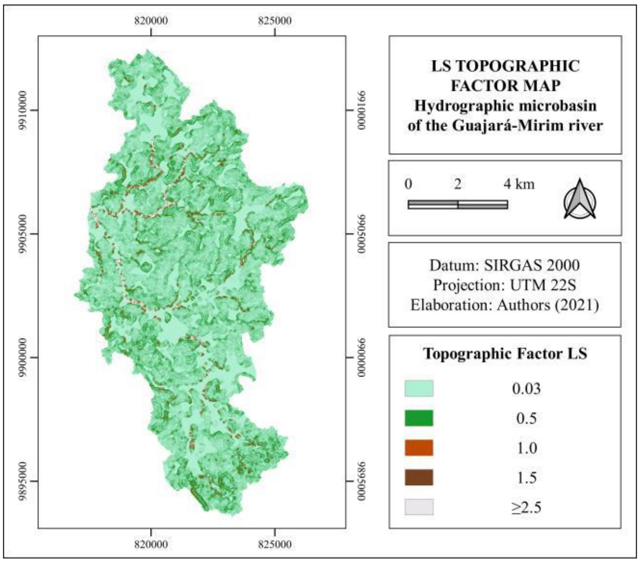


*Fig. 5. LS Topographic Factor Map.*

4.4 Soil Cover Factor (C)

For factor C, different values were used for each land cover class, based on studies by different authors, requiring the correlation of the nomenclature used by these authors with the one adopted in this work [33],[34],[35],[22].

*Table 6. Values for Soil Cover Factor C.*

| Soil Cover | C | Reference |
|---|---|---|
| Anthropized area | 0.000 | Oszoy *et al*. (2012) |
| Hydrography/Weir | 0.000 | Oszoy *et al*. (2012) |
| Native vegetation | 0.001 | Oszoy *et al*. (2012) |
| Secondary vegetation | 0.010 | Oliveira *et al*. (2014) |
| Grass | 0.038 | Oszoy *et al*. 2012 |
| Pasture | 0.090 | Oszoy *et al*. (2012) |
| Agriculture | 0.290 | Beskow *et al*. (2009) |
| Deforestation | 0.404 | Bertoni, Lombardi Netto (2012) |
| Sand extraction | 1.000 | Oszoy *et al*. (2012) |

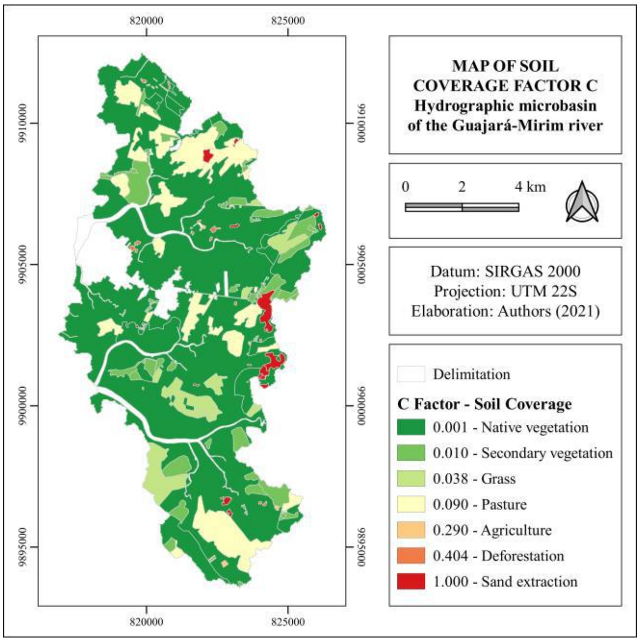


*Fig. 6. Land Cover C Factor Map.*

The areas of the blank map represent the classes of anthropized area, hydrography and dams, for which the literature determines that the value 0.000 (zero) for the C factor of land use should be used. Therefore, they will not be considered as having the potential for rainfall erosion in the USLE [33].

Much of the area of the Guajará-Mirim river watershed is covered by native and secondary vegetation, evidencing the rural characteristic of the municipality. In contrast, there are considerable areas of pasture that are used in local agriculture [13]

With less expressiveness in territorial extension, few areas of agriculture were verified in the microbasin. Having the greatest negative environmental impact, the areas of mineral extraction of sand and deforestation of vegetation showed the highest values for the C factor of soil cover, since they leave the soil more exposed by removing its surface protection, increasing the erosive potential [22],[33].

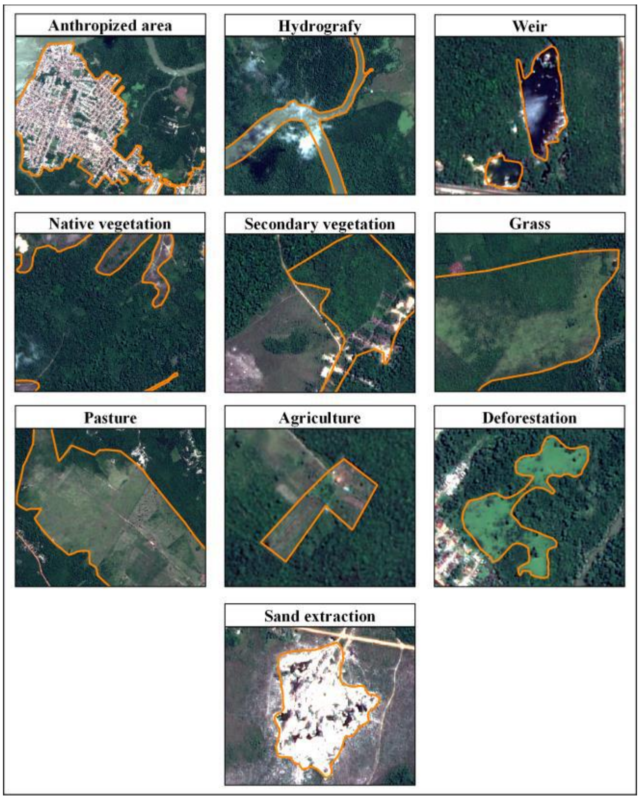


*Fig. 7. land cover classes identified in the study area.*

4.5 Factor of Conservation Practices (P)

In the Guajará-Mirim river watershed, it was not possible to verify the implementation of conservation practices against soil erosion through satellite images, field surveys and literature review [16],[13].

*Table 7. P values for different conservation practices.*

| Conservation practices | P value |
|---|---|
| Planting down the hill | 1.0 |
| Contour planting | 0.5 |
| Alternation of weeding + Contour planting | 0.4 |
| Permanent vegetation string | 0.2 |

*Source: Pruski [36]*

It is inferred that because the study area does not have many hectares of agricultural use currently in activity, is located in a low-altitude region and due to the lack of more active technical monitoring in the area of soil conservation, local rural landowners have not implemented expressively such soil erosion control practices described in the literature, such as contour planting and permanent vegetation cordon [36]. Therefore, a value of 1.0 must be adopted for the P factor of the Universal Soil Persian Equation [4].

4.5 Soil Loss (A)

The Rainfall Erosion Soil Loss Map is the result of multiplying the factors of the Universal Soil Loss Equation, in the form of georeferenced raster files and pre-established numerical values. Thus, each pixel with a spatial resolution of 30 meters has a soil loss value that depends on the characteristics of the area. The multiplication in the Raster Calculator of the RKLS.CP factors generated the map in Figure 8, with the factors R = 682 and P = 1. The physical variables K, LS and C entered as previously processed matrix files [35].

Oliveira et al. [34] developed a classification of intervals to measure the degree of soil loss, in tons per hectare per year, serving as a reference to know how vulnerable the watershed in question is to erosion.

*Table 8. Soil loss classification intervals in tons per hectare per year.*

| Soil loss (t ha$^{-1}$ year$^{-1}$) | Vulnerability |
|---|---|
| 0 – 2.5 | Slight |
| 2.5 – 5 | Slight to Moderate |
| 5 – 10 | Moderate |
| 10 – 15 | Moderate to High |
| 15 – 25 | High |
| 25 – 100 | Very High |
| > 100 | Extremely High |

*Source: Oliveira et al. [34].*

Figure 8 shows a rainfall erosion that varies from mild, in most of the watershed, to moderate, specifically in the sand extraction areas. Table 9 indicates an average soil loss of 1.8381 t.ha$^{-1}$.year$^{-1}$ for the study area, being classified as slight [34].

However, the estimated total soil loss for the entire microbasin area over one year was 249.59 tons of soil. This amount reveals the importance of implementing conservationist practices against erosion, since agribusiness, agriculture, livestock and forest management depend on the quality of the soil. In short, soil degradation harms society in general, as it provides much of what is essential for human and animal life [11].

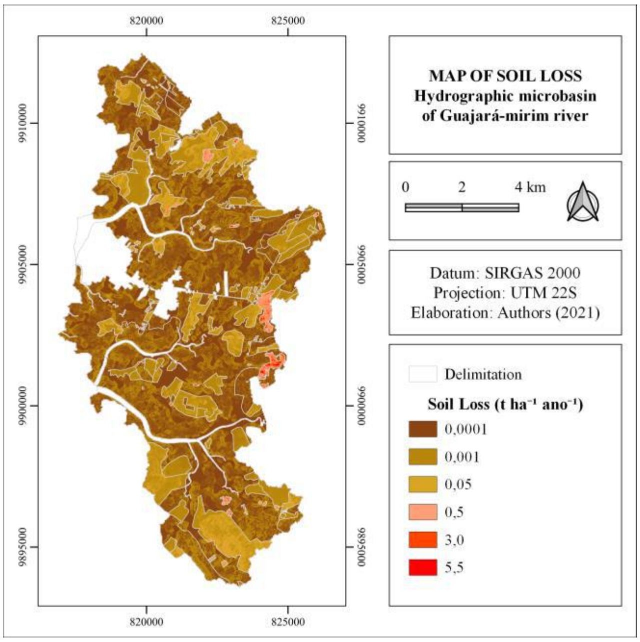


*Fig. 8. Soil Loss Map.*

It is inferred that investments in soil preservation can bring greater returns in a financial and environmental sense, as there are expenses to replace the loss of nutrients that the soil suffers naturally and by anthropic action over time, especially with regard to potential use. agricultural and forestry [37].

It is costly to the environment that rural landowners constantly seek to convert new areas of vegetation for livestock or for logging and mining, when they found degraded the areas they had previously explored [11].

*Table 9. Percentage value of soil loss by cover class.*

| Class | Area (%) | Estimated loss (%) |
|---|---|---|
| 1. Anthropized area | 4.70 | - |
| 2. Hydrography | 3.14 | - |
| 3. Weir | 0.13 | - |
| 4. Agriculture | 0.16 | 0.95 |
| 5. Deforestation | 0.21 | 1.39 |
| 6. Secondary vegetation | 7.11 | 1.52 |
| 7. Native vegetation | 67.43 | 1.80 |
| 8. Grass | 4.43 | 3.01 |
| 9. Pasture | 11.41 | 20.37 |
| 10. Sand extraction | 1.28 | 70.97 |

Table 9 reveals that, despite being the smallest in extent among all land cover classes, the sand mineral extraction category represented the highest percentage amount of erosion for the study area. With the second highest erosive potential, the activity of clean pasture is evident, being the second area in extension of land use in the study area [22].

*Table 10. Soil loss by cover class.*

| Class | Area (ha) | Average Loss ($t\ ha^{-1}\ year^{-1}$) | Estimated Loss ($t\ ano^{-1}$) |
|---|---|---|---|
| 1 | 452.95 | - | - |
| 2 | 302.17 | - | - |
| 3 | 12.49 | - | - |
| 4 | 15.32 | 0.1547 | 2.37 |
| 5 | 19.80 | 0.1749 | 3.46 |
| 6 | 684.91 | 0.0055 | 3.79 |
| 7 | 6496.61 | 0.0007 | 4.48 |
| 8 | 427.06 | 0.0176 | 7.51 |
| 9 | 1099.48 | 0.0462 | 50.83 |
| 10 | 123.15 | 1.4385 | 177.14 |
| | **Total** | **Total** | **Total** |
| | 9633.93 | 1.8381 | 249.59 |

The native vegetation, even with the largest territorial extension in the Guajará-Mirim river watershed, showed a very low soil loss, numerically confirming the importance of vegetation in the control and prevention of soil loss by pluvial erosion [22]

## V. FINAL CONSIDERATIONS

The results show the potential of remote sensing and geotechnologies for soil quality assessment and monitoring. QGIS software is an excellent tool for handling raster and vector data. In it, there was the possibility of classifying the land cover for the study area based on the satellite image CBERS 04A of INPE, in addition to all the geoprocessing procedures described in the methodological part.

The conservation of vegetation and the adoption of erosion control measures are essential to reduce the natural wear and tear that the soil suffers over time. In contrast, the removal of natural vegetation to create pasture areas and the extraction of wood without adequate forest management are causes of soil degradation, as is the mineral extraction of sand. Such practices must be carried out in a sustainable way, combining economic, social and environmental factors.

It is worth mentioning that, whenever possible, there is a greater investment in technical monitoring and scientific research, there is the possibility of carrying out tests to determine specific values of the physical factors of the EUPS, generating more accurate estimates of soil loss. The monitoring of land cover change at regular time intervals by remote sensing is interesting for inspection by environmental agencies, as well as it can meet the interest of research institutions and professionals related to the environmental area.

Finally, the Soil Loss Map is the maximum product that could be elaborated by combining the Universal Soil Loss Equation and the potential of the QGIS geoprocessing software. It is interesting to underline the importance of applying physical equations that can be specialized in order to help professionals who work with the environment to make accurate decisions in their projects.

## REFERENCES

[1] BRASIL. Lei nº 6.938, de 31 de agosto de 1981. (1981). Institui a Política Nacional do Meio Ambiente. Diário Oficial da União. Brasília - DF, 1981.

[2] Lepsch, I.F. (2010). Formação e Conservação dos Solos. Oficina de Textos, 2ª ed., São Paulo – SP.

[3] Pes, L.Z.; giacomini, D.A. (2017). Conservação do solo. Colégio Politécnico da Universidade Federal de Santa Maria.

[4] Wischmeier, W. H.; smith, D. D. Predicting rainfall erosion losses: a guide to conservation planning. (1978). U.S. Department of Agriculture, Agriculture Handbook Nº 537.

[5] Renard, K. G.; Foster, G. A.; Weesies, D. K; Mccool, D. K; Yoder, D. C. (1997). Predicting Soil Erosion by Water: A Guide to Conservation Planning With the Revised Universal Soil Loss Equation (RUSLE). U. S. Department of Agriculture, Agriculture Handbook, n. 703.

[6] Bertoni, J.; Lombardi Neto, F. (2012). Conservação do solo. 8ª ed. São Paulo: Ícone.

[7] Pirovani, D. B.; Silva, A. G.; Santos, A. R.; Cecílio, R. A.; Martins, S. V.; Gleriani, J. M. (2012). Uso de geotecnologias para estudo da fragmentação florestal com base em princípios de ecologia da paisagem. Geotecnologias aplicadas aos recursos florestais, c. 1. Centro de Ciências Agrárias da Universidade Federal do Espírito Santo. Alegre – ES.

[8] Burrough, P.A. (1986). Principles of geographical information systems for land resouces assessment. Oxford, Clarendon Press.

[9] QGIS. Sistema de Informação Geográfica Livre e Aberto. 2021. Available at: <https://qgis.org/pt_BR/site/>.

[10] Zanetti, S. S.; Agrizzi, D. V.; Scárdua, M. D.; Fukunaga, D.; Oliveira, K. D. (2012). Estimativas do escoamento

superficial em uma sub-bacia hidrográfica no município de Rio Novo do Sul, ES. Geotecnologias Aplicadas aos Recursos Florestais. Alegre – ES.
[11] Guerra, A. J. T.; Silva, A. S. Da; Botelho, R. G. M. (2020). Erosão e Conservação dos Solos. Bertrand Brasil, Rio de Janeiro, 11ª ed.
[12] Faustino, J. (1996). Planificación y gestión de manejo de cuencas. Turrialba: CATIE, 1996.
[13] IBGE. (2021b). Instituto Brasileiro de Geografia e Estatística: Portal Cidades. Vigia - Pará. Available at: <https://cidades.ibge.gov.br/brasil/pa/vigia/panorama>.
[14] Kottek M., Grieser J., Beck C., Rudolf B., Rubel F. (2006). World Map of the Köppen-Geiger climate classification updated. Meteorologische Zeitschrift, v.15, n. 3, p.259-263. DOI:10.1127/0941-2948/2013/0507
[15] INPE. (2021a).Instituto Nacional de Pesquisas Espaciais. Divisão de Geração de Imagens. Available at: <http://www2.dgi.inpe.br/catalogo/explore>.
[16] INPE. (2021b). Instituto Nacional de Pesquisas Espaciais. Câmeras Imageadoras CBERS 04A. Available at: <http://www.cbers.inpe.br/sobre/cameras/cbers04a.php>.
[17] INPE. (2021c). Instituto Nacional de Pesquisas Espaciais. Projeto Topodata: Banco de Dados Geomorfométricos do Brasil. Available at: <http://www.dsr.inpe.br/topodata/acesso.php>.
[18] Santos, A. R. (2020a). Pré-processamento - Etapa 03: Correção de valores negativos do MDE SRTM de 30m no QGIS. Available at: <https://youtu.be/h75zqJMMs9A>.
[19] Santos, A. R. (2020b). Pré-processamento - Etapa 04: Preencher pixels sem dados do MDE SRTM de 30m no QGIS. Available at: <https://youtu.be/w5oD56xmWh8>.
[20] Santos, A. R. (2020c). Pré-processamento - Etapa 05: Remoção de depressões espúrias do MDE SRTM de 30m no QGIS. Available at: <https://youtu.be/1J2TR50oTZU>.
[21] SAGA. GIS Module Library Documentation: Module LS Factor, Field Based. 2021. Available at: <www.saga-gis.org/saga_tool_doc/2.2.7/ta_hydrology_25.html>.
[22] Lombardi Neto, F.; Moldenhauer, W. C. (1992). Erosividade da chuva: sua distribuição e relação com as perdas de solo em Campinas (SP). Bragantia, v. 51, n. 2.
[23] ANA. (2021). Agência Nacional de Águas. *Sistema Nacional de Informações sobre Recursos Hídricos (SNIRH).* Available at: <https://www.snirh.gov.br/hidroweb/serieshistoricas>. Acesso em: 14 jul.
[24] IBGE. (2006). Instituto Brasileiro de Geografia e Estatística: Mapa de Solos do Brasil.
[25] CPRM. (2010). Serviço Geológico Do Brasil. Mapa Geodiversidade do Estado do Pará. https://rigeo.cprm.gov.br/handle/doc/14705.
[26] Freeman, G. T. (1991). Calculating catchment area with divergent flow based on a regular grid. Computers and Geosciences, 17:413-22.
[27] Desmet, P. J. J.; Govers, G. (1996). A GIS Procedure for Automatically Calculating the USLE LS Factor on Topographically Complex Landscape Units. Journal of Soil and Water Conservation, 51 (5), 427-433.
[28] ESRI. (2020). Esri 10-Meter Land Cover: A 10-meter resolution map of Earth’s land surface from. Available at: <https://livingatlas.arcgis.com/landcover/>.
[29] TERRASCLASS. (2021). GeoPortal TerraClass - Amazônia Legal. Available at: <https://www.terraclass.gov.br/geoportal-aml/>.
[30] Silva, A. M.; Schulz, H. E.; Camargo, P.B. (2003). Erosão e hidrossedimentologia em bacias hidrográficas. São Carlos: RiMa.
[31] Silva, A. M.; Alvares, C. A. (2005). Levantamento de informações e estruturação de um banco de dados sobre a erodibilidade de classes de solos no Estado de São Paulo. Geociências, Rio Claro, v. 24, n. 1.
[32] EMBRAPA. (1979). Empresa Brasileira de Pesquisa Agropecuária. Súmula da 10 - Reunião Técnica de Levantamento de Solos. Serviço Nacional de Levantamento e Conservação de Solos. Rio de Janeiro.
[33] Oszoy, G.; Aksoy, E.; Dirim, M. S.; Tumsavas, Z. (2012). Determination of soil erosion risk in the Mustafakemalpasa River Basin, Turkey, using the Revised Universal Soil Loss Equation, Geographic Information System, and Remote Sensing. Environmental Management. 50(4):679- 694.
[34] Oliveira, V. A.; Mello, C. R.; Durães, M. F.; Silva, A. M. (2014). Vulnerabilidade dos solos à erosão hídrica na bacia hidrográfica do Rio Verde, sul de Minas Gerais. Ciência e Agrotecnologia, Universidade Federal de Lavras, v. 38, n. 3, p. 262-269.
[35] Beskow, S.; Mello, C.R.; Norton, L. D. (2009). Soil erosion prediction in the Grande River Basin, Brazil using distributed modeling. Catena. 79(1):49-59.
[36] Pruski, F. F. (2009). Conservação de solo e água: Práticas mecânicas para o controle da erosão hídrica. Viçosa: Ed. Viçosa.
[37] Paiva, J. B. D.; Paiva, E. M C. D. (2003. Hidrologia Aplicada à Gestão de Pequenas Bacias Hidrográficas. FINEP, ABRH, Porto Alegre.